ESJ Natural/Life/Medical Sciences

Petrographic and Geochemical Characteristics of the Djabatoure Massif Metamagmatites from the Pan-African Orogen in Central Togo, West Africa

Sarakawa Abalo Malibida Kpanzou, PhD
Department of Geology, Faculty of Sciences, University of Lomé, Togo.
Department of Civil Engineering, Laboratory of Geotechnics and Mining,
Regional Training Center for Road Maintenance
(CERFER - Entente Council), Lomé, Togo
Gnanwasou Alayi
Yao Agbossoumondé
Mahaman Sani Tairou
Department of Geology, Faculty of Sciences, University of Lomé, Togo
José María González-Jiménez
Instituto Andaluz de Ciencias de la Tierra,
CSIC-Universidad de Granada, Granada, Spain
Antonio *Garcia-Casco*
Departamento de Mineralogía y Petrología,
Universidad de Granada, Granada, Spain

Doi:10.19044/esj.2023.v19n24p198

Submitted: 21 July 2023
Accepted: 28 August 2023
Published: 31 August 2023

Cite As:
Kpanzou S.A.M., Alayi G., Agbossoumondé Y., Tairou M.S., González-Jiménez J.M. & Garcia-Casco A. (2023). *Petrographic and Geochemical Characteristics of the Djabatoure Massif Metamagmatites from the Pan-African Orogen in Central Togo, West Africa*. European Scientific Journal, ESJ, 19 (24), 198. https://doi.org/10.19044/esj.2023.v19n24p198

Abstract

The Dahomeyide orogen, in Togo and adjoining parts of southeast Ghana and Benin, represents the suture of West Africa Craton (WAC) into northwest Gondwana. The suture zone corresponds to a narrow and lithologically diverse area with high pressure granulite complexes. The Djabatoure massif, located in the central part of Togo, belongs to the suture zone. The aim of this paper is to present the petrographic and geochemical characteristics of the Djabatoure massif in order to better understand the geodynamic evolution of the Dahomeyide belt in Togo. The methodology

 ISSN: 1857-7881 (Print) e - ISSN 1857-7431

implemented is based on a synthesis of previous works, a petrographic study of 20 thin sections, and a geochemical study through discrimination diagrams of 15 rock samples. Results show that the Djabatoure massif is composed of granulites, pyroxenites, amphibolites, talcschists and gneisses. These rocks were equilibrated under granulite facies conditions and subsequently partially retrogressed to the amphibolite facies. The Djabatoure massif rocks also display tholeiitic affinity, enriched LREE, and negative anomalies in Nb, Zr and Ti; all these characteristics indicate subduction zone magmtism. These features are consistent with protoliths of tholeiites, N-MORB, and volcanic arc basalts affinities. The Djabatoure massif rocks were emplaced in an oceanic environment and likely originated from a metasomatized mantle.

Keywords: Petrography, Geochemistry, Djabatoure massif, Pan-African orogen, West Africa

Introduction

In the Pan-African Dahomeyide belt, the basic to ultrabasic complexes of Derouvarou (Benin), Kabye-Kpaza, Djabatoure-Anie, Agou-Ahito (Togo), and Shaï or Akuse (Ghana) form a submeridian mountainous belt materializing the suture zone (Ménot and Séddoh, 1980; Agbossoumondé, 1998; Attoh, 1998; Agbossoumondé et al., 2001; Tairou and Affaton, 2013). The Djabatoure massif, located in the central part of Togo, represents one of the most remarkable morphostructures of this belt. It is defined, like the other massifs of this suture zone, as a highly metamagmatic ophiolitic-type unit. It is composed of ultramafic, gabbroic metacumulates, metagabbros, metadolerites, metabasalts, pyroxenites, amphibolites and granulites (Ménot, 1977, 1980, 1982; Ménot and Seddoh, 1980; Agbossoumondé, 1998; Duclaux, 2003; Agbossoumondé et al, 2007; Kpanzou, 2017, 2023; Kpanzou et al., 2019, 2022). Previous studies (Duclaux, 2003; Sabi, 2007; Agbossoumondé et al., 2007) have partially addressed the petrographic and geochemical characteristics of all the massifs of the togolese segment of the suture zone. According to these studies, the Djabatoure massif is composed of dolerites and gabbros, and is formed by several episodes of magma injections into the migmatitic basement of the Touareg Shield. The Djabatoure massif shows a signature of continental tholeiite emplaced in the continental crust and slow cooling during exhumation. It is also believed that the rocks of Djabatoure massif underwent metamorphism in the granulite facies with a retrogression in the amphibolite facies associated with the nappes emplacement. These are metaluminous rocks with a tholeiitic signature emplaced in a continental or oceanic arc context and exhumed during the Pan-African tangential phase.

Despite efforts to better understand the petrography and geochemistry of the Djabatoure massif metamagmatites, detailed petrographic and

 ISSN: 1857-7881 (Print) e - ISSN 1857-7431

geochemical characterization of the rocks of this massif remains are lacking. Therefore, the present study is a contribution to the detailed petrographic and geochemical study of the Djabatoure massif metamagmatites. Specifically, the study aims to provide (i) a detailed petrographic description of the Djabatoure metamagmatites, (ii) a rock classification and origin, (iii) and geodynamic environment.

1. Geological context

The Pan-African Dahomeyide belt resulted from the collision between 3 structures: the eastern portion of the WAC, the Benino-Nigerian basement, and the Touareg Shield (Caby et al., 1981; Attoh et al., 1997; Ganade de Araujo et al., 2014a). It is subdivided into three structural zones which are from west to east: the external zone, the suture zone, and the internal zone (Affaton, 1990) (Figure 1).

The external zone corresponds to the Buem and Atacora structural units. The Buem is composed of metasedimentary rocks that originated from the metamorphism of the Volta Basin units. The Atacora consists of orthogneissic units of Kara-Niamtougou and the granitoids of the Kpalimé-Amlamé pluton (Affaton, 1990; Affaton et al, 1991; Agbossoumondé et al., 2007; Tairou et al., 2009; Aidoo et al., 2020; Kwayisi et al., 2021; Tairou et al., 2022). The external zone overlaps the WAC and its sedimentary cover.

The suture zone is materialized by a submeridian alignment of complexes: Derouvarou in Benin, Kabye-Kpaza, Djabatoure-Anie, and Agou-Ahito in Togo, and Akuse or Shaï in Ghana. These complexes are composed of mafic to ultramafic rocks (granulite or sometimes eclogite facies), witnesses of the Pan-African crustal thickening (Ménot and Séddoh, 1985; Attoh, 1998; Agbossoumondé et al., 2001; Attoh and Morgan, 2004; Aidoo et al., 2020; Kpanzou, 2023).

The internal zone is a peneplain representing the remobilized Benin-Nigerian shield (BNS) in the Pan-African belt (Affaton, 1990). It is composed of gneisso-migmatitic, metasedimentary (schists, marbles, and quartzites), and Pan-African granitoid units (Affaton et al., 1991; Caby and Boessé, 2001; Alayi, 2018).

 ISSN: 1857-7881 (Print) e - ISSN 1857-7431

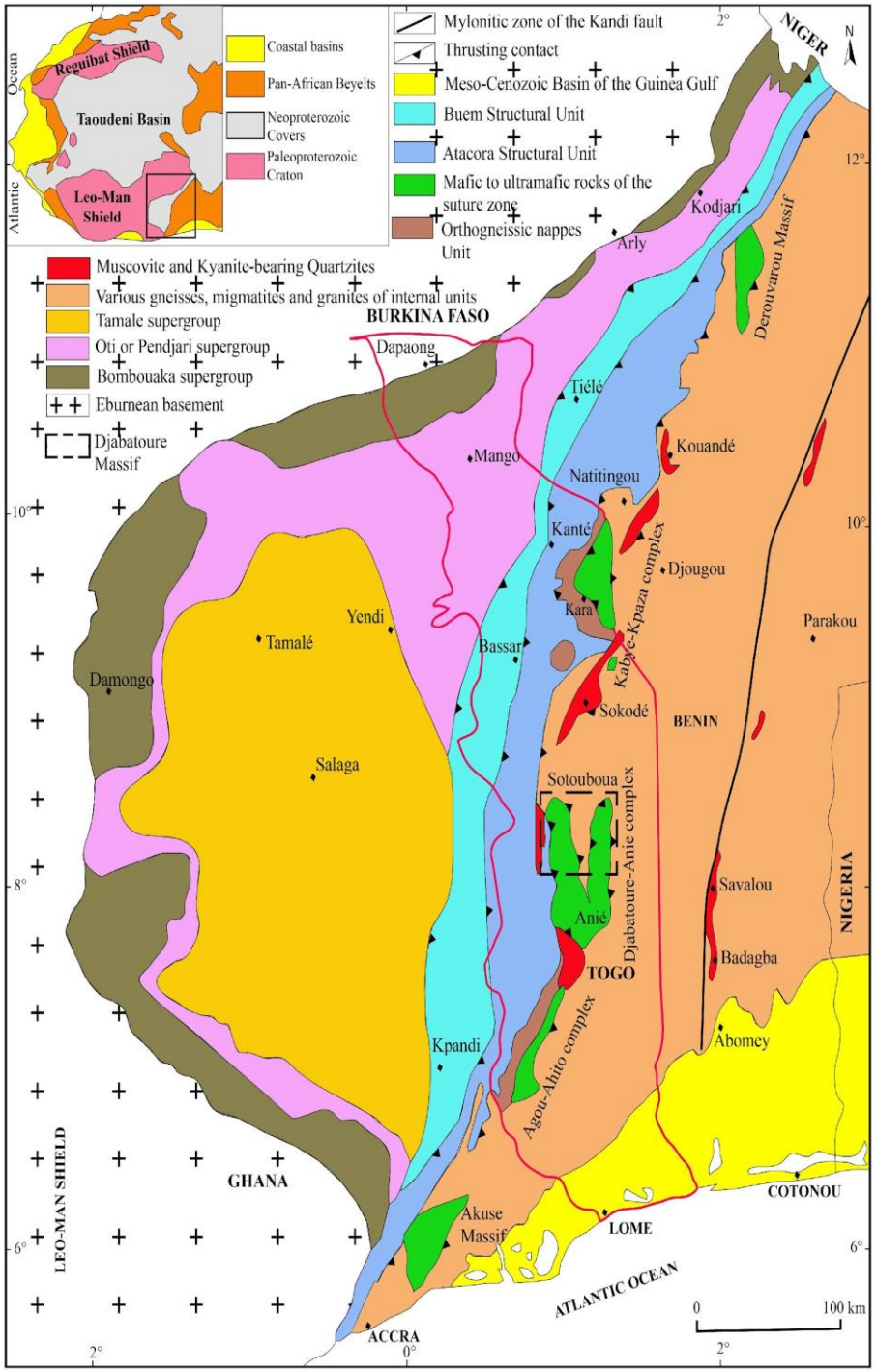

Figure 1. Simplified geologic map showing the main structural domains of the Pan-African Dahomeyide belt and its foreland (Affaton, 1990; slightly modified) with the location of the Djabatoure massif

 ISSN: 1857-7881 (Print) e - ISSN 1857-7431

2. Methodology

This study is based on a literature review of previous work, fieldwork, laboratory analysis, data processing, and analysis. The literature review allowed for a synthesis of previous work on the regional and/or local geology of the study area. The field campaign allowed us to take 50 samples and describe them in a macroscopic way. We georeferenced the outcrops and sampling stations using a Garmin eTrex Legend H GPS. Twenty (20) thin sections were made to determine textural and mineralogical compositions. We selected fifteen (15) samples for whole-rock analysis performed at the Centre for Scientific Instrumentation of the University of Granada (CIC-UGR) in Spain. The analytical approach adopted is as follows:

- (i) Major elements oxides were determined with a Philips Magix Pro (Pw-2440) X-ray fluorescence (XRF) equipment after melting the rock sample in a solution with tetra lithium borate. The characteristic precision as determined from standards AN-G and BEN, was better than ± 1.5 % (relative error) for an analyte concentration of 10 wt.%. The iron content is expressed as FeO* total. The molar ratio MgO/(MgO+FeO*) is abbreviated Mg#. Zirconium was determined with the same instrument using the same glass beads; with a precision better than ± 0.2% for 5 ppm Zr. Loss on Ignition (LOI) was determined by weight difference before and after ignition of samples in a furnace. In the diagrams, oxide concentrations are reported on an anhydrous (volatile-free) basis.
- (ii) Trace elements, except Zr, were determined by an Inductively Coupled Plasma-Mass Spectrometry (ICP-MS) after HNO_3 + HF digestion of 0.1000 g of sample powder in a Teflon-lined vessel at 180°C and 200 psi for 30 min, evaporation to dryness and subsequent dissolution in 100 ml of 4 vol.% HNO_3; the precision, as determined from standards PMS, WSE, UBN, BEN, BR and AGV run as unknowns, was better than ± 2% for analyte concentrations of 50 ppm and ± 5% for analyte concentrations of 5 ppm.

The results of the chemical analyses are reported in Table 1. The location of the analyzed samples is shown in Figure 2. Field and chemical data were compiled in Excel and imported into different software (GCD kit, QGIS …) for specific processing. For the geochemical data processing, we proceeded to the normalization of major elements to 100% under anhydrous basis.

3. Results

3.1. Petrography

The Djabatoure massif metamagmatites (Figure 2) are essentially composed of granulites (garnet-bearing or garnet-free), pyroxenites, amphibolites, talcschists and gneisses (garnet-bearing or garnet-free). Representative rock samples were selected for petrographic studies to determine the textures and mineralogical compositions.

 ISSN: 1857-7881 (Print) e - ISSN 1857-7431

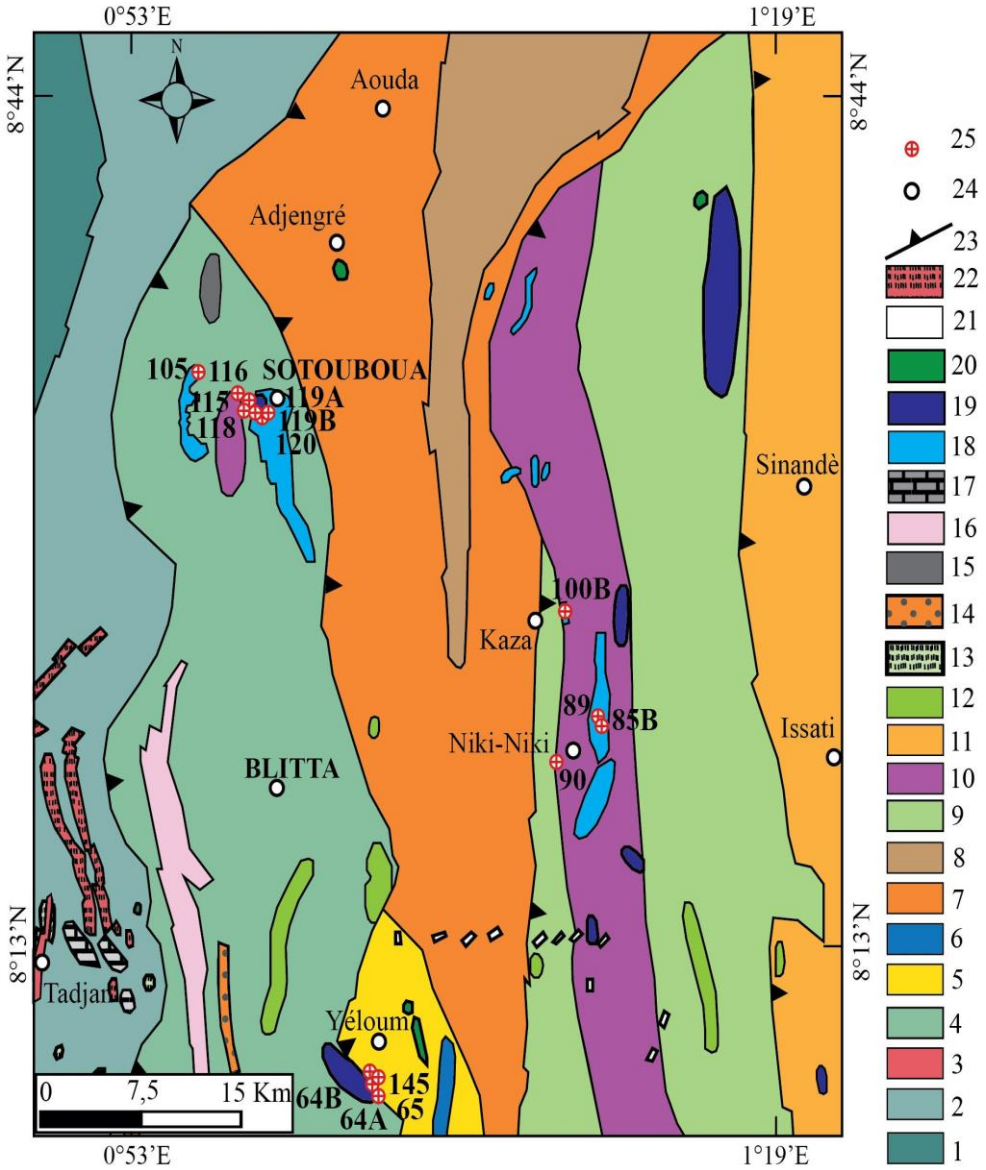

Figure 2. Schematic map of the Djabatoure massif showing the location of the samples analyzed (modified from the geological map of Sylvain et al., 1986).

1: micaschists and graphitic schists; 2: sericite- and chlorite-bearing schists; 3: feldspathic quartzites; 4: garnet-bearing gneiss; 5: 2-mica-bearing paragneiss; 6: biotite-bearing micaschists; 7 : 2-mica-bearing gneiss; 8: kyanite- and garnet-bearing gneiss; 9: biotite- and amphibole-bearing gneiss; 10: clear metagabbroic granulites; 11: 2-mica- and amphibole-bearing gneiss; 12: amphibolites; 13 : Metavolcanites and associated albitic schists; 14: tectonized feldspathic quartzites; 15: basic charnockitic orthogneisses; 16: kyanite-bearing quartzites; 17: crystalline dolomites (marbles); 18: dark metagabbroic granulites; 19: pyroxenites; 20: serpentinites; 21: quartz veins; 22: muscovite- and or sericite-bearing quartzites; 23: overlapping contact; 24: towns and villages; 25: samples.

 ISSN: 1857-7881 (Print) e - ISSN 1857-7431

3.1.1. Granulites

The granulites observed and described in the field are of two types: garnet-free granulites and garnet-bearing granulites.

3.1.1.1. Garnet-free granulites

They outcrop at Sotouboua, Niki-Niki, and Yeloum massifs. They are cut into milky white to grayish banks and balls (Figure 3a). Microscopically, they show granoblastic to double coronite textures (Figure 3b). The coronites are evidence of re-equilibration reactions between plagioclase and pyroxene blasts. Reactions in which clinopyroxene develops in the crown around orthopyroxene and amphibole in that around plagioclase. These reactions of re-equilibration often take place in the context of pressure and rather high temperature. The essential minerals are plagioclase, clinopyroxene, orthopyroxene, and amphibole. Plagioclases are more abundant in phenocrysts with polysynthetic twins and more or less clear rolling extinction. Orthopyroxenes (hypersthene) are deformed and show numerous cleavages, microfractures undulate extinction. Clinopyroxenes (diopside) occur as slightly microfractured or intensely cracked subautomorphic blasts, either as small crystals in the internal crown around the orthopyroxene. Amphiboles in elongated subautomorphic phenocrysts contain oxide inclusions. They are generally very little represented and constitute either early minerals in the form of large patches associated with pyroxenes or acicular minerals forming crowns around orthopyroxenes. Quartz is quite rare and occurs in xenomorphic form in inclusion in plagioclase and amphibole.

3.1.1.2. Garnet-bearing granulites

They are observed at Sotouboua massif. They are homogeneous, with a foliation of alternating light quartzo-feldspathic and dark amphibole and pyroxene layers, to which are added numerous millimetric to centimetric garnets, reddish in veinlets and wire rods (Figure 3c). Microscopically, they have a granoblastic texture consisting of plagioclase, pyroxene (orthopyroxene), amphibole, and garnet (Figure 3d). Plagioclase is abundant and exists as xenomorphic and sometimes automorphic phenocrysts with polysynthetic macles. Orthopyroxene (hypersthene) is subautomorphic with strong relief and nearly orthogonal cleavages. Amphibole (hornblende) is scarce and occurs in small, more or less elongated sections of bluish green to brown color. Garnet is subautomorphic to automorphic and sometimes globular. It is very abundant in ferromagnesian beds and contains inclusions of quartz, plagioclase, epidote, and opaque minerals (ilmenite, rutile, and magnetite).

 ISSN: 1857-7881 (Print) e - ISSN 1857-7431

3.1.2. Pyroxenites

They outcrop at Sotouboua, Niki-Niki, and Yeloum massifs. They are often cumulated with coarse or medium grains of pyroxene (Figure 3e). They are dark gray to black, massive in structure, and flow in very dense balls. Microscopically, they display a granoblastic texture made of jointed pyroxenes, with green hornblende crystallized at their borders (Figure 3f). They are mainly composed of clinopyroxene, orthopyroxene, and amphibole. Clinopyroxenes (diopside) are the most abundant. They are slightly colored in green and show numerous cracks and undulate extinction. Orthopyroxenes (hypersthene) are pinkish colored with undulate extinction. They are much cleaved and contain inclusions of opaque minerals (ilmenite, rutile, and magnetite). Amphiboles (green hornblende) are elongated phenocrysts joined to pyroxenes. They also constitute small crystals forming a reaction crown around orthopyroxenes (the result of the reaction between orthopyroxenes and clinopyroxenes).

Figure 3. Macroscopic (a, c, and e) and microscopic (b, d, and f) photography of the Djabatoure massif rocks. (a and b): coronite garnet-free granulite; (c and d): garnet-bearing granulite; (e and f): pyroxenite. Opx: orthopyroxene; Cpx: clinopyroxene; Pl: plagioclase; Hbl: hornblende; Grt: garnet.

 ISSN: 1857-7881 (Print) e - ISSN 1857-7431

3.1.3. Amphibolites

They are observed at Sotouboua and Yeloum massifs. They are dark grey rocks, with a foliated structure and fine grains that are cut into platelets. On the field, they are crossed by veinlets and quartzo-feldspathic wire rods (Figure 4a). Microscopically, they have a nematogranoblastic texture with amphibole, plagioclase and quartz minerals (Figure 4b). Amphibole is represented by green hornblende in elongated bluish-green or brownish elongated sections. Plagioclase is more or less abundant and present polysynthetic twin. Quartz, with rolling extinction, is not very abundant and is found in association with plagioclase in the clear beds.

3.1.4. Talcschists

They outcrop in balls at Niki-Niki massif. They are milky white to greenish, with a schistose or foliated structure (Figure 4c). Microscopically, they have a porphyroblastic texture with phenoblasts of clinopyroxene, talc, and serpentine (Figure 4d). Clinopyroxene (diopside) occurs as intensely cracked phenocrysts. It sometimes recrystallizes into amphibole or serpentine and contains inclusions of opaque minerals (magnetite). Talc, often associated with chlorite is from retromorphosis of amphiboles.

3.1.5. Garnet-bearing gneiss

These are mostly amphibole- and garnet-bearing gneisses that outcrop around granulites. They are grayish, of foliated structure, and with millimetric to centimetric garnets (Figure 4e). Microscopically, they show a granoblastic texture composed of feldspars, quartz, biotite, amphibole, and garnet (Figure 4f). Feldspars are subautomorphic and polysynthetic twins. Quartz shows undulate extinction. Amphibole (green hornblende) forms elongated, cracked blasts with opaque mineral inclusions. Garnets in automorphic porphyroblasts are often cracked and contain inclusions of feldspars, quartz, and oxides.

 ISSN: 1857-7881 (Print) e - ISSN 1857-7431

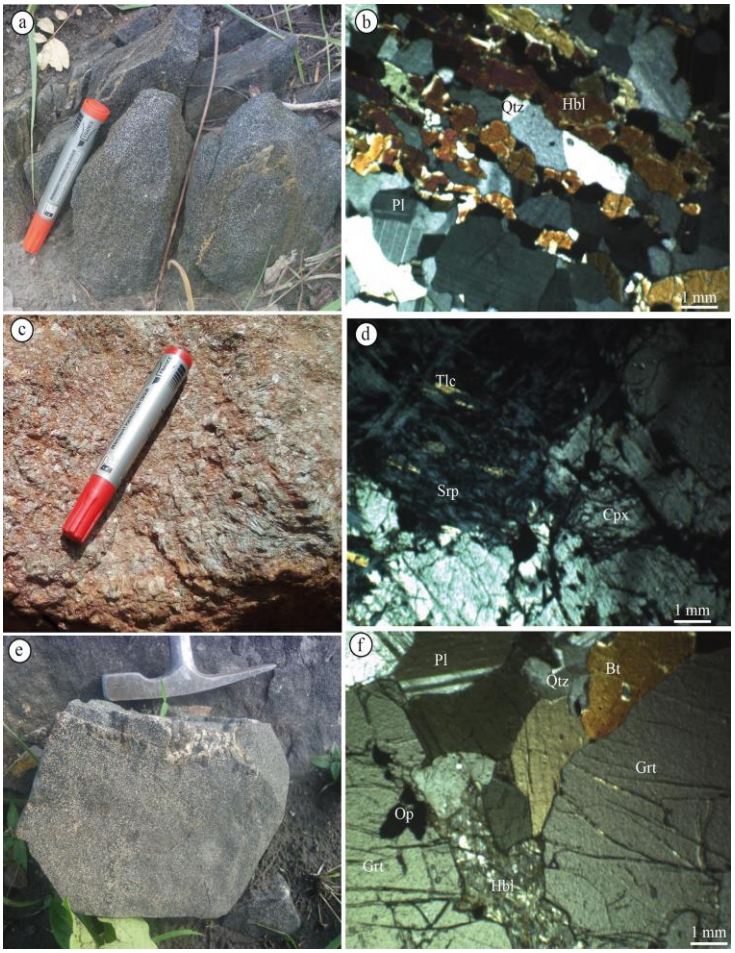

Figure 4. Macroscopic (a, c, and e) and microscopic (b, d, and f) photography of the Djabatoure massif rocks. (a and b): amphibolite; (c and d): talcschist; (e and f): garnet-bearing gneiss. Qtz: quartz; Pl: plagioclase; Cpx: clinopyroxene; Hbl: hornblende; Bt: biotite; Grt: garnet; Srp: serpentine; Tlc: talc; Op: opaque.

3.2. Geochemistry

3.2.1. Major Elements Distribution

The Djabatoure massif rocks are characterized by silica contents in the range of 40.26% to 54.14% (Table 1). They are mainly granulites, pyroxenites, and amphibolites. The analyzed samples show high values of Al_2O_3 up to 21.34% and Sr up to 580.91 ppm, which implies their richness in plagioclase. MgO contents reach 19.14% and Fe_2O_3 up to 13.97% indicating pyroxene accumulation.

According to Harker diagrams (Figure 5): granulites show a positive correlation between SiO_2 vs TiO_2, FeOt, Na_2O, K_2O, P_2O_5 and negative with Al_2O_3, MgO, and CaO; pyroxenites show a positive correlation between SiO_2 vs MgO and negative with Al_2O_3, TiO_2, CaO, Na_2O, K_2O, and P_2O_5;

 ISSN: 1857-7881 (Print) e - ISSN 1857-7431

amphibolites show a positive correlation between SiO_2 vs Na_2O, K_2O, P_2O_5 and negative with Al_2O_3, TiO_2, FeOt, and CaO.

Table 1. Results of geochemical analyses of major elements (%), trace elements (ppm), and rare earth elements (ppm) of the Djabatoure massif rocks.

Lithology	Granulites								Pyroxenites					Amphibolites	
Ech.	85B	89	90	105	115	118	119A	120	64A	64B	100B	116	145	65	119B
Xcoord.	E1°12'01,9"	E1°11'51,3"	E1°10'10,8"	E0°55'28,6"	E0°57'42,8"	E0°57'05,3"	E0°58'15,8"	E0°58'08,3"	E1°02'36,3"	E1°02'36,3"	E1°10'31,1"	E0°58'01,4"	E1°02'31,4"	E1°02'45,7"	E0°58'15,8"
Ycoord.	N8°21'12,1"	N8°21'48,9"	N8°20'04,1"	N8°34'12,4"	N8°33'10,8"	N8°33'25,1"	N8°32'48,8"	N8°32'37,4"	N8°08'23,1"	N8°08'23,1"	N8°25'33,1"	N8°33'10,3"	N8°08'39,9"	N8°08'09,9"	N8°32'48,8"
Majors (%)															
SiO2	50,64	51,86	49,42	54,14	49,70	50,34	47,80	48,73	47,05	51,86	49,10	47,76	52,36	50,33	40,26
Al2O3	7,90	17,09	16,60	17,88	18,89	14,69	19,83	18,20	9,85	5,16	15,09	7,56	6,55	14,71	21,34
Fe2O3	8,74	6,94	10,87	9,55	7,49	12,20	7,74	7,86	10,81	9,12	9,00	10,69	11,45	12,54	13,97
MnO	0,15	0,12	0,14	0,15	0,12	0,27	0,11	0,12	0,17	0,14	0,15	0,21	0,19	0,21	0,11
MgO	13,76	9,63	6,19	4,09	6,48	8,80	10,52	9,98	14,60	19,14	10,90	15,44	17,52	6,59	6,83
CaO	16,05	10,37	9,29	8,43	12,82	9,99	11,27	11,48	12,54	10,95	11,87	14,85	10,34	9,38	12,27
Na2O	0,81	2,51	2,70	3,40	2,82	2,28	2,24	2,44	1,73	0,78	1,43	1,24	0,98	3,25	2,00
K2O	0,16	0,20	0,88	0,49	0,17	0,17	0,04	0,07	0,36	0,10	0,33	0,11	0,05	0,23	0,11
TiO2	0,59	0,38	1,18	1,17	0,67	0,93	0,24	0,28	1,19	0,55	0,71	0,93	0,51	1,47	1,73
P2O5	0,02	0,04	0,30	0,23	0,08	0,16	0,02	0,02	0,10	0,03	0,07	0,02	0,02	0,13	0,03
PAF	0,62	0,45	1,92	0,00	0,68	0,00	0,00	0,23	1,02	1,74	0,90	0,53	0,02	0,80	0,74
Total	**99,44**	**99,59**	**99,49**	**99,53**	**99,92**	**99,83**	**99,81**	**99,41**	**99,42**	**99,57**	**99,55**	**99,34**	**99,99**	**99,64**	**99,39**
Traces (ppm)															
Rb	4,89	3,29	19,61	3,37	1,96	1,56	0,14	0,44	2,23	0,67	5,52	0,34	0,57	4,15	0,28
Ba	42,72	96,26	240,35	215,04	53,30	82,83	20,91	77,80	54,42	49,18	85,92	36,66	67,11	49,98	26,93
Nb	1,14	1,15	2,67	5,26	1,80	3,87	0,84	0,76	2,66	1,24	2,26	1,30	1,24	2,50	1,38
Ta	0,08	0,09	0,16	0,37	0,15	1,49	0,28	0,07	0,15	0,05	0,14	0,08	0,47	0,19	0,15
Sr	166,39	418,23	580,91	438,62	355,62	298,91	300,27	284,90	113,94	55,10	377,78	117,89	130,85	162,12	514,87
Zr	35,50	25,00	90,20	80,00	35,60	35,60	13,60	14,40	39,50	24,80	51,00	23,10	24,00	81,60	27,50
Y	19,38	7,89	18,26	20,17	11,55	18,83	3,18	5,17	18,76	12,60	14,32	16,32	12,01	30,74	13,31
Hf	1,07	0,28	0,75	0,57	0,32	0,46	0,00	0,00	1,28	0,49	0,68	0,59	0,52	0,64	0,41
Ni	359,76	189,36	64,01	16,84	71,98	116,29	200,46	214,46	497,54	580,30	150,51	338,84	580,91	34,14	92,97
Cr	2269,25	363,63	123,63	33,90	270,92	440,88	317,29	355,17	949,85	1715,01	233,42	1842,86	939,15	15,49	18,09
V	248,01	113,08	304,38	226,53	136,56	164,86	49,45	74,89	298,24	195,28	173,92	187,78	205,31	314,93	452,41
U	0,13	0,04	0,17	0,12	0,04	0,05	0,00	0,00	0,16	0,07	0,09	0,01	0,02	0,11	0,00
Th	0,00	0,00	0,01	0,00	0,00	0,00	0,00	0,00	0,00	0,00	0,00	0,00	0,00	0,00	0,00
Sc	56,84	22,83	26,48	24,54	29,01	41,09	17,17	25,04	50,07	46,48	39,15	47,41	40,57	41,16	27,83
Co	60,92	53,13	49,84	54,77	46,19	208,01	94,81	66,41	65,34	67,64	60,35	64,71	130,98	57,99	82,66
Cu	123,64	24,76	87,87	17,75	18,77	48,78	42,29	95,65	151,20	80,19	119,31	94,97	194,70	69,17	204,36
Zn	49,25	50,18	85,15	84,18	44,19	108,90	38,99	38,98	76,52	59,47	66,72	67,19	71,18	91,75	72,77
Mo	1,77	2,84	2,55	5,10	2,68	2,91	3,69	2,38	1,77	1,31	2,46	2,28	2,89	2,43	2,17
Cs	0,33	0,24	0,53	0,14	0,12	0,12	0,08	0,08	0,09	0,10	0,34	0,06	0,08	0,12	0,08
Li	6,91	5,42	8,72	8,23	2,64	2,98	0,00	0,57	2,79	1,08	9,47	0,43	1,44	6,39	0,79
Be	0,30	0,37	0,78	0,97	0,34	0,54	0,21	0,21	0,43	0,28	0,40	0,21	0,30	0,63	0,24
Ga	10,13	14,29	20,14	20,64	17,71	15,10	14,57	15,18	14,12	7,65	14,38	10,29	9,41	16,83	20,87
Sn	0,37	0,03	0,71	0,33	0,16	0,38	0,00	0,00	0,71	0,23	0,35	0,32	0,24	0,63	0,37
Tl	0,04	0,03	0,09	0,03	0,03	0,03	0,02	0,04	0,03	0,02	0,04	0,02	0,02	0,04	0,02
Pb	0,65	1,30	3,56	3,70	1,43	1,62	0,10	0,16	0,59	0,45	1,68	0,00	0,29	1,65	0,22
REE (ppm)															
La	4,98	3,64	10,67	10,52	3,40	5,65	0,72	0,68	7,23	3,54	4,99	3,03	2,48	5,24	2,43
Ce	12,86	7,44	25,12	23,70	8,34	13,06	1,86	1,83	18,68	8,95	11,75	7,91	6,49	13,52	6,30
Pr	1,95	1,01	3,51	3,20	1,21	1,90	0,27	0,30	2,83	1,34	1,68	1,30	1,11	1,92	1,02
Nd	9,57	4,70	16,24	14,86	6,12	9,58	1,41	1,65	14,58	6,92	8,27	7,62	5,95	10,08	5,55
Sm	3,00	1,22	3,89	3,71	1,77	2,80	0,39	0,55	3,95	2,03	2,31	2,74	1,84	3,30	2,07
Eu	0,93	0,38	1,29	1,23	0,50	0,85	0,12	0,20	1,28	0,58	0,81	0,77	0,63	1,08	0,67
Gd	2,48	1,19	2,94	2,98	1,46	2,33	0,42	0,64	3,06	1,55	2,39	2,30	1,99	3,78	1,87
Tb	0,46	0,21	0,46	0,50	0,26	0,43	0,07	0,11	0,51	0,29	0,36	0,40	0,33	0,68	0,34
Dy	2,96	1,27	2,85	3,09	1,75	2,82	0,57	0,76	3,04	1,92	2,18	2,61	1,81	4,42	2,19
Ho	0,64	0,28	0,60	0,66	0,40	0,62	0,14	0,20	0,63	0,43	0,48	0,55	0,41	0,99	0,46
Er	1,64	0,86	1,52	1,69	1,07	1,64	0,42	0,65	1,58	1,18	1,31	1,42	1,15	2,47	1,20
Tm	0,24	0,14	0,22	0,25	0,16	0,25	0,07	0,11	0,23	0,18	0,20	0,21	0,18	0,36	0,18
Yb	1,43	0,87	1,32	1,49	0,99	1,50	0,39	0,66	1,32	1,07	1,17	1,19	1,05	2,18	0,99
Lu	0,21	0,13	0,19	0,23	0,14	0,23	0,06	0,09	0,19	0,15	0,17	0,17	0,16	0,33	0,14
Eu/Eu*	1,02	0,94	1,14	1,11	0,93	1,00	0,89	1,01	1,10	0,98	1,03	0,92	0,99	0,92	1,02
(La)N	12,97	9,48	27,79	27,40	8,85	14,71	1,88	1,77	18,83	9,22	12,99	7,89	6,46	13,65	6,33
(Sm)N	12,95	5,27	16,80	16,02	7,64	12,09	1,68	2,37	17,06	8,77	9,97	11,83	7,95	14,25	8,94
(Gd)N	8,09	3,88	9,59	9,72	4,76	7,60	1,37	2,09	9,98	5,06	7,80	7,50	6,49	12,33	6,10
(Yb)N	6,22	3,78	5,74	6,48	4,30	6,52	1,70	2,87	5,74	4,65	5,09	5,17	4,57	9,48	4,30
(La/Sm)N	1,00	1,80	1,65	1,71	1,16	1,22	1,11	0,75	1,10	1,05	1,30	0,67	0,81	0,96	0,71
(Gd/Yb)N	1,30	1,03	1,67	1,50	1,11	1,17	0,81	0,73	1,74	1,09	1,53	1,45	1,42	1,30	1,42
(La/Yb)N	2,09	2,51	4,84	4,23	2,06	2,26	1,11	0,62	3,28	1,98	2,55	1,53	1,41	1,44	1,47
ΣREE	43,35	23,34	70,82	68,11	27,57	43,66	6,91	8,43	59,11	30,13	38,07	32,22	25,58	50,35	25,41

 ISSN: 1857-7881 (Print) e - ISSN 1857-7431

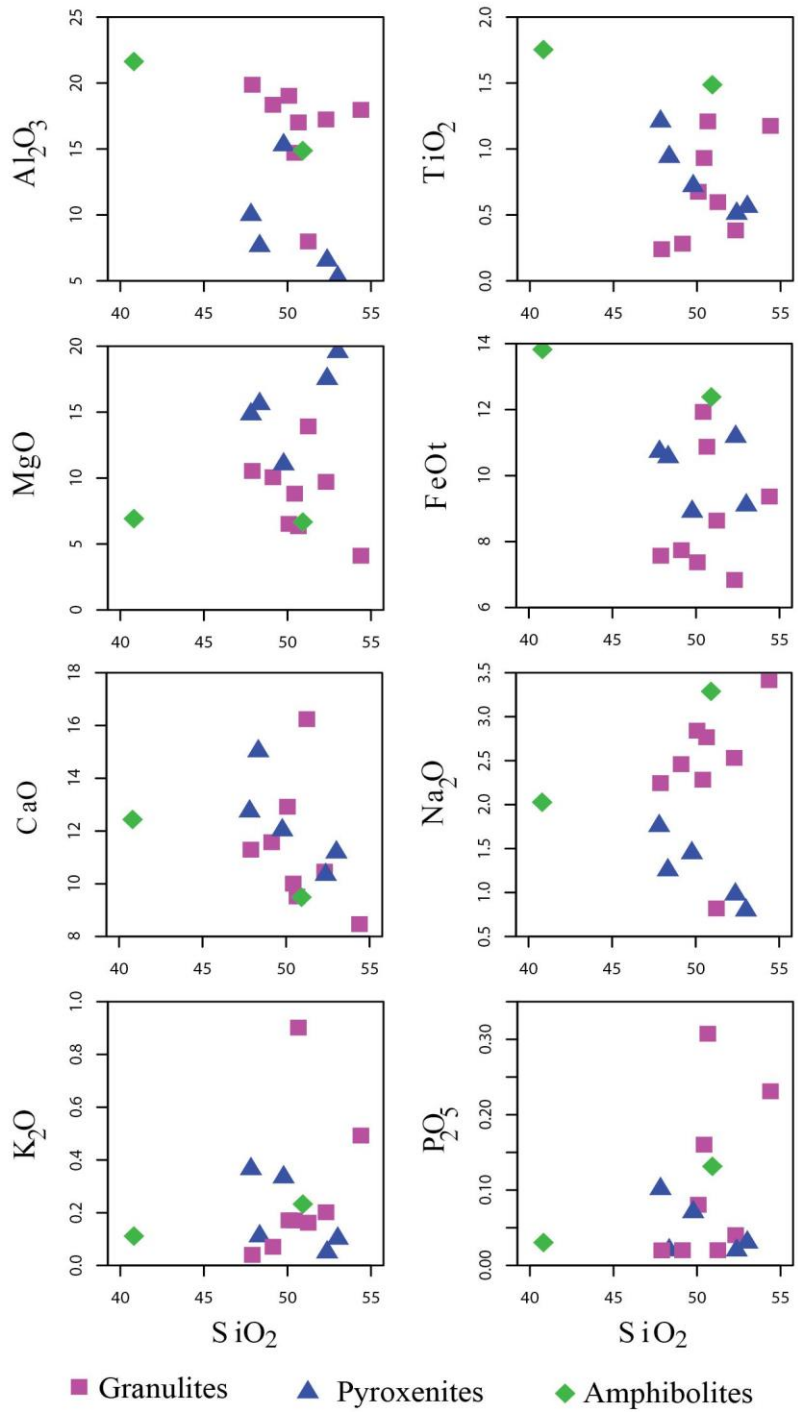

Figure 5. Oxides (TiO_2, FeOt, Na_2O, K_2O, P_2O_5, Al_2O_3, MgO, CaO) vs SiO_2 variation diagrams in Djabatoure massif rocks (Harker, 1909).

 ISSN: 1857-7881 (Print) e - ISSN 1857-7431

3.2.2. Traces and rare earth elements distribution

In the trace elements (Rb, Sr, Nd, Ba, Nb, Y, Ni, Cr) versus Zr diagrams (Harker, 1909) (Figure 6): granulites show a positive correlation between Zr vs Rb, Sr, Nd, Ba, Nb, Y and negative with Ni and Cr; pyroxenites show a positive correlation between Zr vs Rb, Sr, Nd, Ba, Nb, Y and negative with Ni and Cr; amphibolites show a positive correlation between Zr vs Rb, Nd, Ba, Nb, Y and negative with Sr and Ni.

Rare earth spectra normalized to chondrites (Nakamura, 1974) (Figure 7a) show that the rocks of the Djabatoure massif are moderately fractionated ($0.62 \leq (La/Yb)N \leq 4.84$). They are slightly rich in light rare earth elements ($0.67 \leq (La/Sm)N \leq 1.80$) and show generally flat heavy rare earth elements spectra ($0.73 \leq (Gd/Yb)N \leq 1.74$). These rocks record positive anomalies in Pr, Ho, Tm and negative in Ce, Nd, Gd, Dy, Er, Yb.

Multielement spectra normalized to the early mantle (McDonough and Sun, 1995) (Figure 7b) show that the rocks of the Djabatoure massif have positive anomalies in Ba, Ta, Sm, Y, and negative in Rb, U, Nb, Pb, Zr.

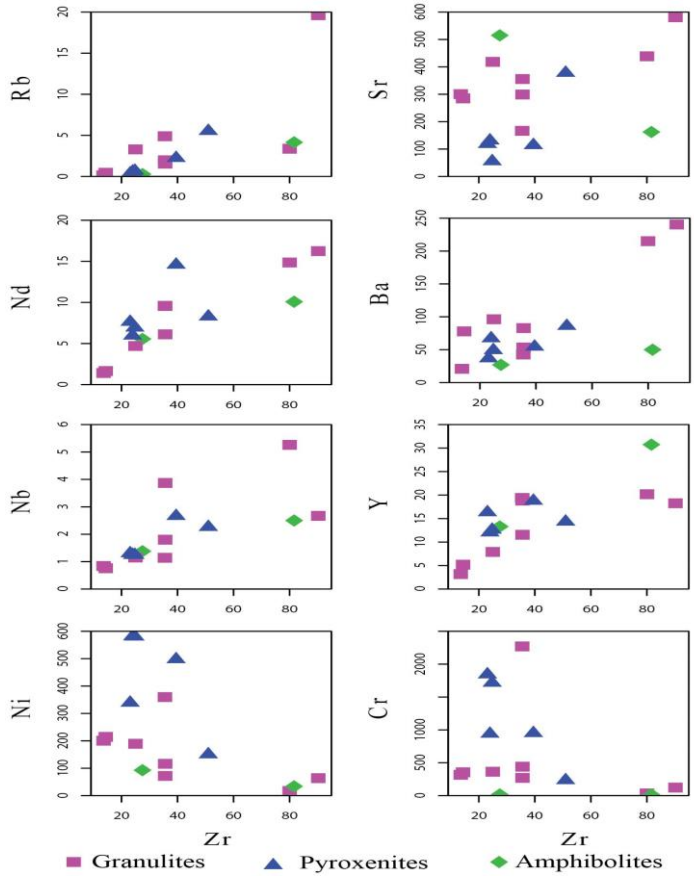

Figure 6. Traces elements (Rb, Sr, Nd, Ba, Nb, Y, Ni, Cr) versus Zr variation diagrams in Djabatoure massif rocks (Harker, 1909).

 ISSN: 1857-7881 (Print) e - ISSN 1857-7431

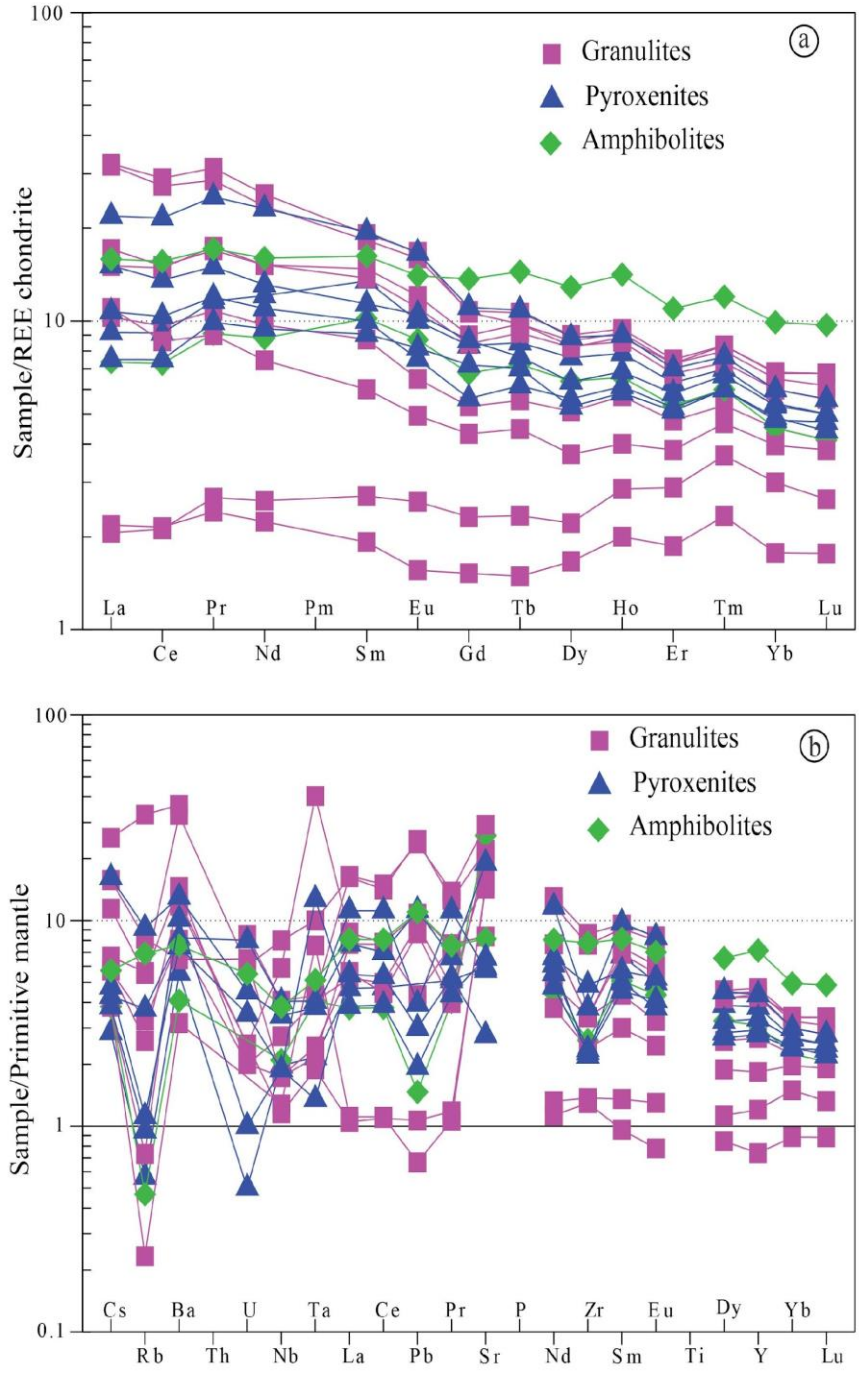

Figure 7. (a) Rare earth elements spectra normalized to chondrites (Nakamura, 1974) and (b) trace elements spectra normalized to the primitive mantle (McDonough and Sun, 1995) of the Djabatoure massif rocks.

 ISSN: 1857-7881 (Print) e - ISSN 1857-7431

3.2.3. Type of the rocks and geodynamic context

The Djabatoure massif rocks are distributed in the TAS diagram of Middlemost (1994) (Figure 8a) in the gabbroic diorites and gabbros fields. The diagram of Irvine and Baragar (1971) (Figure 8b) indicates that the rocks of this massif have a tholeiitic affinity. The diagram of Shand (1943) (Figure 8c) shows that these rocks are metaluminous. The Meschede (1986) diagram (Figure 8d) shows that the rocks of the Djabatoure massif fall into two domains: N-MORB (D), and intraplate tholeiitic and volcanic arc basalts (C).

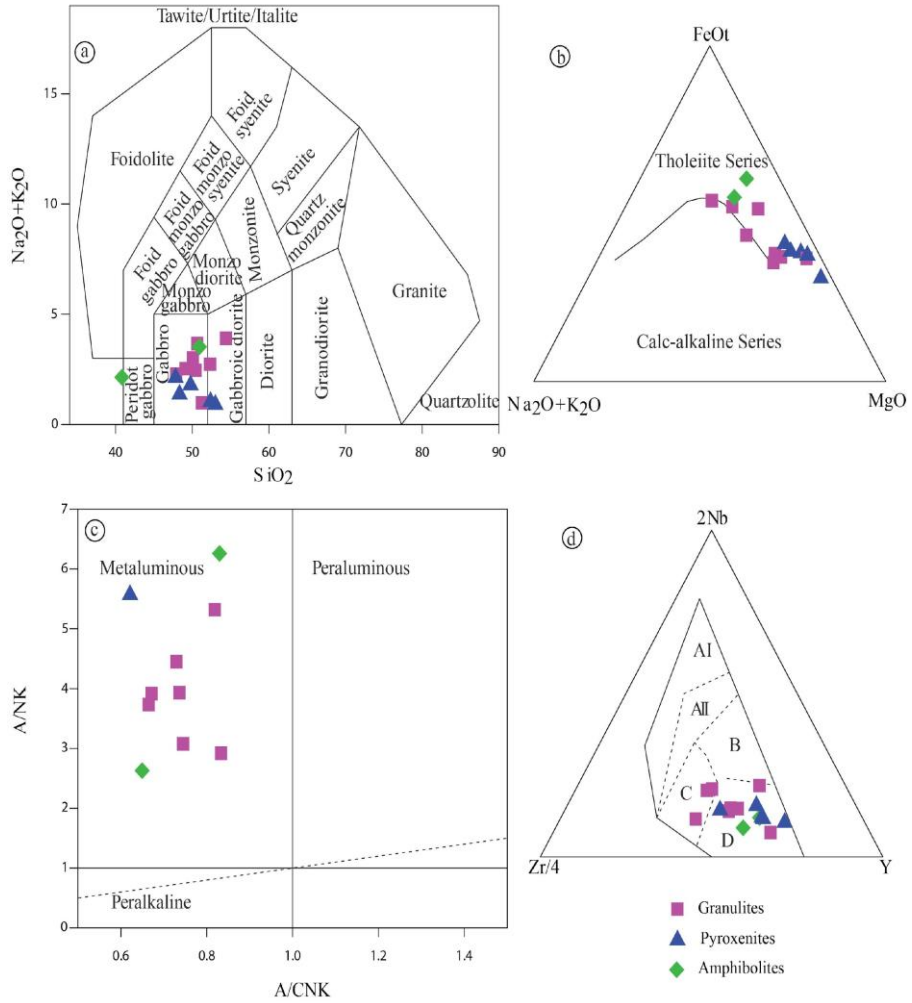

Figure 8. Geochemical classification plots of Djabatoure massif rocks. (a): Na_2O+K_2O vs SiO_2 (Middlemost, 1994); (b): FeOt-(Na_2O+K_2O)-MgO (Irvine and Baragar, 1971); (c): A/NK vs A/CNK (Shand, 1943); (c): Zr/4-Nb-Y (Meschede, 1986) [AI = intraplate alkaline basalts; AII = intraplate alkaline basalts and tholeiites; B = E-type MORB; C = intraplate tholeiites and volcanic arc basalts; D = N-type MORB].

 ISSN: 1857-7881 (Print) e - ISSN 1857-7431

4. Discussion

4.1. Petrography and metamorphic evolution

The petrographic study of the Djabatoure massif shows a diversity of rocks: granulites, pyroxenites, talcschists, amphibolites, and gneisses. The different mineralogical associations of the samples described are presented in Table 2. They show the different metamorphic episodes that affected these rocks.

Coronitic granulites are generally garnet-free. Coronitic textures are the result of reactions between plagioclases and orthopyroxenes in which clinopyroxene develops in the crowns around orthopyroxenes and amphiboles in those around plagioclases. This amphibole crown is late and results from the hydration of clinopyroxenes. The clinopyroxenes crown is the result of the reaction between plagioclases and orthopyroxenes, while the amphiboles crown is late and the result of the hydration of clinopyroxènes (Sabi et al., 2015; Agbossoumondé et al., 2017; Guillot et al., 2019; Kpanzou, 2023).
Garnet-bearing granulites represent facies without coronites. They are characterized by the mineralogical assemblage of Pl+Opx+Hbl+Grt.
Amphibolitization has led to the transformation of granulites (garnet-free or bearing-garnet) into amphibolites characterized by the Hbl+Pl+Qtz paragenesis, indicating the transition from granulite facies to amphibolite facies.

The pyroxenites have an Opx+Cpx+Pl+Hbl paragenesis and underwent a first retromorphosis in the amphibolite facies, with the replacement of pyroxenes by green hornblende, and a second one in the greenschist facies which led to serpentinization and talcschization (Sabi, 2007; Agbossoumondé et al., 2017; Guillot et al., 2019; Boukaoud et al., 2021; Tairou et al., 2022).

The garnet gneisses present mineralogical associations with Pl+Qtz+Bt+Hbl+Grt witnessing a high-grade metamorphism with the presence of garnet in their composition.

Table 2. Mineralogical composition of the petrographic facies of the Djabatouré massif

Petrographic facies	Main minerals	Accessory minerals
Garnet-free granulites	Pl+Cpx+Opx+Hbl	Ep+Opaque
Garnet-bearing granulites	Pl+Opx+Hbl+Grt	Opaque
Pyroxenites	Opx+Cpx+Pl+Hbl	Opaque
Amphibolites	Hbl+Pl+Qtz	Ep+Opaque
Talcschists	Cpx+Srp+Tlc	Ep+Opaque
Garnet-bearing gneiss	Pl+Qtz+Bt+Hbl+Grt	Opaque

 ISSN: 1857-7881 (Print) e - ISSN 1857-7431

4.2. Fractional crystallization

The correlations observed in the Harker variation diagrams of major and trace elements, the parallelism of rare earth elements spectra and multi-element spectra, indicate an evolution of the different facies from the unique magmatic source.

The slight negative anomalies Nb-Ta and the enrichment in Rb and Ba imply the influence of recycling of crustal material (crustal contamination). The positive anomaly in Sr suggests plagioclase accumulation. The good linear correlation in the Harker diagrams reflects the intervention of a differentiation process by fractional crystallization in the evolution of the parent magmas of these massif rocks.

The increase of FeOt versus SiO_2 in the granulites indicates the accumulation of opaque minerals such as magnetite and ilmenite. The negative correlation of MgO vs SiO_2 in the granulites shows the fractionation of pyroxene and amphibole in these rocks. The increase of Na_2O and K_2O versus SiO_2 in granulites and amphibolites indicates their richness in acid plagioclase. The increase in P_2O_5 in granulites and amphibolites is indicative of either apatite crystallization or fluid circulation. The decrease of Al_2O_3 and CaO vs SiO_2 in granulites and amphibolites marks an early crystallization of calcium plagioclase in the least evolved terms. The negative correlation of MgO and CaO versus silica in granulites reflects the simultaneous fractionation of olivine, pyroxene, and plagioclase in primary magmas (Guillot et al., 2019; Tairou et al., 2022; Kpanzou, 2023).

The increase in Rb and Ba contents suggests the high fractionation of plagioclase in these rocks. The decrease in Ni and Cr contents vs. Zr is consistent with the fractionation of ferromagnesians (pyroxene and amphibole) in these rocks. These elements could also be associated with MgO and FeOt in pyroxenes (Hamlaoui et al., 2020; Kpanzou, 2023).

4.3. Source of magmas

The Djabatoure massif metamagmatites have an intermediate to ultrabasic composition. They have mineralogical and chemical characteristics that allow them to be classified as gabbros and gabbroic diorites according to the terminology of Middlemost (1994). The petrographic characteristics reflect the chemical composition of these rocks with the abundance of hornblende, the presence of orthopyroxene and clinopyroxene, as well as apatite as accessory mineral. Negative anomalies of elements such as niobium, phosphorus and titanium, observed on the multielement spectra are fingerprints commonly attributed to subduction zone magmas. The negative anomaly in Nb is characteristic of continental tholeiites and of crustal contamination or metasomatism from a mantle source (Guillot et al., 2019; Kpanzou et al., 2022; Tairou et al., 2022; Kpanzou, 2023).

 ISSN: 1857-7881 (Print) e - ISSN 1857-7431

The genesis of these rocks is therefore compatible with emplacement in a magmatic arc context with simultaneous crustal assimilation and fractional crystallisation of magma probably derived from continental crust.

4.4. Geotectonic environment

Based on the petrogeochemical data of the Djabatoure massif metamagmatites, such as the tholeiitic affinity rocks with metaluminous signature, it can be proposed that they were emplaced in a probably extensive tectonic context (Duclaux, 2003; Guillot et al., 2019; Kpanzou et al., 2022). Geotectonic discrimination diagrams indicate that these rocks were emplaced in various contexts: intraplate tholéiites, N-MORB and volcanic arc basalts. The negative anomaly Nb is characteristic of continental tholeiites and crustal contamination. It suggests a context of subduction zones in which Nb is trapped.

The Djabatoure massif rocks have similar geochemical characteristics to those of the Kabye and Agou massifs, such as high Sr and Ba values, a negative anomaly in Nb, and enrichment in light rare earth elements (LREE) compared to heavy rare earth elements (HREE) (Sabi, 20007; Sabi et al., 2015; Agbossoumondé et al., 2017). The rocks of this massif have been classified as typical late-orogenic magmas probably derived from a mantle source, enriched, metasomatized by plunging plate fluids and subducted sediments during a subduction event (Affaton, 1990; Agbossoumondé, 1998; Duclaux, 2003; Sabi, 2007) and subsequently contaminated by the continental crust (Agbossoumondé et al., 2017; Liégeois, 2019; Aidoo et al., 2020; Kpanzou, 2023).

Despite the lack of isotopic data, the analogies of petrogeochemical studies of the rocks of the Djabatoure massif with those of the Kabye and Agou massifs allow them to be classified in the same geodynamic context.

Conclusion

Petrographic studies of the Djabatoure massif have identified: granulites, amphibolites, and gneisses representing foliated facies; massive to cumulative pyroxenites; schistose to laminated talcschists. Most of these rocks present mineralogies dominated by a primary paragenesis constituted by an abundance of plagioclase followed by clinopyroxene and a secondary paragenesis which is mainly represented by alteration minerals such as amphibole iron and titanium oxides. This paragenesis shows that these rocks underwent metamorphism in the granulite facies with a retrogression in the amphibolite facies. Thus, the massif has undergone a metamorphic evolution from granulitization to retromorphosis in the amphibolite facies.

Geochemical characterization shows that the rocks of the Djabatoure massif display metaluminous and tholeiitic affinity. Inter-element variations

 ISSN: 1857-7881 (Print) e - ISSN 1857-7431

indicate that these rocks evolved from a fractional crystallization process accompanied by crustal contamination. They were emplaced in various settings: intraplate tholéiites, N-MORB, and volcanic arc basalts. They are crustal base rocks uplifted by Pan-African tectonics in crustal sets. Geochemical trends clearly indicate emplacement in a subduction context.

The Djabatoure massif rocks show enrichment in LREE compared to HREE and sub-flat HREE spectra. The multi-element spectra show that most of the rocks are rich in mobile elements (Rb, Sr, and Ba) and have negative anomalies in Nb, P, and Ti. These characteristics are similar to those of rocks from a mantle source enriched and metasomatized during a subduction event.

Acknowledgements

I would like to thank the authorities of the universities of the Coimbra Group who, through the "Coimbra Group Short Stay Scholarship Programme for young researchers from Sub-Saharan Africa", has granted me a laboratory research scholarship for the realization of geochemical analyses of rock samples. I also thank Professors Antonio GARCIA-CASCO and José María GONZÁLEZ-JIMÉNEZ, both professors-researchers at the Department of Petrology and Mineralogy of the University of Granada in Spain, who agreed to support my application for the scholarship and to carry out the chemical analyses of my rock samples in their laboratory. We acknowledge the anonymous reviewers for their constructive comments which improve the quality of the initial manuscript.

Data Availability: All of the data are included in the content of the paper.

Conflicts of interest: The authors have no conflicts of interest to declare.

References:

1. Affaton, P. (1990). Le bassin des Volta (Afrique de l´Ouest) : une marge passive d´âge protérozoïque supérieur, tectonisée au Panafricain (600±50 Ma). Edit. ORSTOM, Collection Etudes & Thèses, Paris, 500p. https://horizon.documentation.ird.fr/exl-doc/pleins_textes/pleins_textes_2/etudes_theses/31718.pdf
2. Affaton, P., Gelard, J.P., Simpara, N. (1991). Paléocontraintes enregistrées par la fracturation dans l'unité structurale de l'Atacora (Chaîne Panafricaine des Dahomeyides, Togo). C. R. Acad. Sci., Paris, t. 312 : 763-768.
http://pascal-francis.inist.fr/vibad/index.php?action=getRecordDetail&idt=19679359

 ISSN: 1857-7881 (Print) e - ISSN 1857-7431

3. Agbossoumondé, Y. (1998). Les complexes ultrabasiques de la chaîne panafricaine au Togo (Axe Agou – Atakpamé, Sud-Togo). Etude pétrographique, minéralogique et géochimique. Thèse Doct. Lab. Géol. Pétro. Univ. Jean Monnet St. Etienne Fr., 306p.
4. Agbossoumondé, Y., Ménot, R.-P., Guillot, S. (2001). Metamorphic evolution of Neoproterozoic eclogites from South Togo (West Africa). Jour. of Afr. Earth Sc. https://doi.org/10.1016/S0899-5362(01)80061-0 33, 227–244.
5. Agbossoumondé, Y., Ménot, R.-P., Paquette, J.L., Guillot, S., Yéssoufou, S., Perrache, C. (2007). Petrological and geochronological constraints on the origin of the Palimé–Amlamé granitoids (South Togo, West Africa): A segment of the West African Craton Paleoproterozoic margin reactivated during the Pan-African collision. Gondwana Research 12, 476-488. https://doi.org/10.1016/j.gr.2007.01.004
6. Agbossoumondé, Y., Ménot, R. P., Ganade de Araujo, C. E. (2017). Major, Trace Elements and Sr-Nd Isotopic Characteristics of High-Pressure and Associated Metabasites from the Pan-African Suture Zone of Southern Togo, West Africa. *Journal of Environment and Earth Science*, ISSN 2225-0948, Vol.7, No.2. https://iiste.org/Journals/index.php/JEES/article/view/35429
7. Aidoo, F., Sub, F.-Y., Liang, T., Nude, P.M. (2020). New insight into the Dahomeyide Belt of southeastern Ghana, West Africa: Evidence of arc-continental collision and Neoarchaean crustal reworking. Precambrian Research 347 (2020) 105836. https://doi.org/10.1016/j.precamres.2020.105836.
8. Alayi, G. (2018). Les granitoïdes tardifs de la chaîne panafricaine des Dahomeyides au Togo: étude pétro-structurale, géochimique et géochronologique. Thèse Doctorat, FDS, Univ. Lomé-Togo, 256p.
9. Attoh, K. (1998). High-Pressure Granulite Facies metamorphism in the Pan-African Dahomeyide orogen, West Africa. J. Geology, 106 : 236-246. https://doi.org/10.1086/516019
10. Attoh, K., Dallmeyer, R.D., Affaton, P. (1997). Chronology of nappe assembly in the Pan-Africa Dahomeyide Orogen, West Africa: evidence from 40Ar/39Ar mineral ages. Precambrian research, 82, pp. 153 – 171. https://doi.org/10.1016/S0301-9268(96)00031-9
11. Attoh, K., Morgan, J. (2004). Geochemistry of high-pressure granulites from the Pan-African Dahomeyide orogen, West Africa: constraints on the origin and composition of lower crust. Jour.of Afr.Earth Sci., vol. 39, pp. 201-208. https://doi.org/10.1016/j.jafrearsci.2004.07.048

 ISSN: 1857-7881 (Print) e - ISSN 1857-7431

12. Boukaoud, E. H., Godard, G., Chabou, M. C., Bouftouha, Y., & Doukkari, S. (2021). Petrology and geochemistry of the Texenna ophiolites, northeastern Algeria: Implications for the Maghrebian flysch suture zone. Lithos 390, 106019. https://apps.umc.edu.dz/vrp/virtualseminar/doc/Proceeding_Magmatism_Precambrian_bases_petrography.pdf
13. Caby, R., Bertrand, J.M., Black, R. (1981). Pan-African closure and continental collision in the Hoggar. Ifora segment, central Sahara. In Kröner A. (Eds) Precambrian Plate Tectorics. Elsevier, Amst, pp. 407-434. https://www.scirp.org/%28S%28351jmbntvnsjt1aadkozje%29%29/reference/referencespapers.aspx?referenceid=1160492
14. Caby, R., Boessé, J.M. (2001). Pan–African nappe system in southwest Nigeria: the Ife– Ilesha schist belt. Jour.of Afr.Earth Sci., vol. 33 n°2, pp. 211- 225. DOI : 10.1016/S0899-5362(01)80060-9
15. Duclaux, G. (2003). Etude pétrologique et structurale des massifs basiques et ultrabasiques de la zone de suture panafricaine de la chaîne des Dahomeyides au Togo : Implications géodynamiques. Mém. DEA, Lab. Dyn. Lithos. Univ. J. Monnet, St-Etienne, 29p. https://doi.org/10.13140/RG.2.2.28332.92809
16. Ganade de Araujo, C.E., Rubatto, D., Hermann, J., Cordani, U.G., Caby, R., Basei, M.A.S. (2014a). Ediacaran 2,500-km-long synchronous deep continental subduction in the West Gondwana Orogen. Nature Communications, 5:5198. doi: 10.1038/ncomms6198.
17. Guillot, S., Agbossoumondé, Y., Bascou, J., Berger, J., Duclaux, G., Ménot, R.P., Schwartz, S. (2019). Transition from subduction to collision recorded in the Pan-African arc Complexes (Mali to Ghana). *Precambr. Res.* 320, 261–280. https://doi.org/10.1016/j.precamres.2018.11.007
18. Hamlaoui, H., Laouar, R., Bouhle, S., Boyce, A. J. (2020). Caractéristiques pétrologiques et géochimiques des roches magmatiques d'El Aouana, NE algérien". *Estudios Geológicos enero-junio*, e124 ISSN-L: 0367-0449, 76(1). https://doi.org/10.3989/egeol.43391.510
19. Harker, A. (1909). The natural history of igneous Rocks. Methuen and Co., London, 384p. https://doi.org/10.1017/CBO9780511920424
20. Irvine, T.N., Baragar, W.R.A. (1971). A guide to chemical classification of the common volcanic rocks. Can. J. Earth Sci., 8: 523-548. https://doi.org/10.1139/e71-055
21. Kpanzou, S.A.M. (2017). Etude pétrographique et structurale du massif de Djabatouré et des massifs adjacents. Mém. Master, FDS, Univ. Lomé, 31p.

 ISSN: 1857-7881 (Print) e - ISSN 1857-7431

22. Kpanzou, S.A.M. (2023). Contribution à l'étude du complexe basique-ultrabasique de Djabatouré-Anié (Centre-Togo) : Caractéristiques pétrostructurales, géochimiques et indices de minéralisations associés. Thèse de Doctorat unique, FDS, Univ. Lomé, 232p.
23. Kpanzou, S.A.M., Agbossoumondé, Y., Tairou, M.S. (2019). Caractérisation pétrostructurale du massif granulitique de Djabatouré. J. Rech. Sci. Univ. Lomé (Togo), Spécial 2019, 21(4-2) : 509-519. https://www.ajol.info/index.php/jrsul/article/view/206992
24. Kpanzou, S.A.M., Agbossoumondé, Y., González Jiménez, J.M., Tairou, M.S., Garcia-Casco, A. (2022). Pétrologie et métallogénie des indices de Ni-Cr associés au massif basique-ultrabasique de Oké, Togo. Afrique SCIENCE 21(1) : 53-69. https://www.afriquescience.net/PDF/21/1/5.pdf
25. Kwayisi, D., Elburg, M., Lehmann, J. (2021). Preserved ancient oceanic lithosphere within the Buem structural unit at the eastern margin of the west African craton, LITHOS (2021), https://doi.org/10.1016/j.lithos.2021.106585
26. Liégeois, J.P. (2019). New synthetic Geological Map of the Tuareg shield: An Overview of its Global structure and Geological Evolution. Springer, Geology Switzerland, 83p. https://apps.umc.edu.dz/vrp/virtualseminar/doc/Proceeding_Magmatism_Precambrian_bases_petrography.pdf
27. McDonough, W.F., Sun, S.S. (1995). The composition of the Earth. Chemical Geology 120, pp. 223–253. https://doi.org/10.1016/0009-2541(94)00140-4
28. Ménot, R.-P. (1977). Les massifs basiques et ultrabasiques antémétamorphiques de la bordure Ouest du mole Dahoméo-nigérian. Essai de synthèse bibliographique. Ann. Univ. Bénin, Lomé, pp. 53-94. https://www.researchgate.net/publication/327822999
29. Ménot, R.-P. (1980). Les massifs basiques et ultrabasiques de la zone mobile panafricaine au Ghana, Togo et au Bénin. Etat de la question. Bull. soc. Géol. Fr., 7 : 297-303. https://doi.org/10.2113/gssgfbull.S7-XXII.3.297
30. Ménot, R.-P. (1982). Les éclogites des Monts Lato : un témoin de l'évolution tectono-métamorphique de la chaîne pan-africaine du Togo (Afrique de l'Ouest). Ist. intern. Eclogite Conf., Terra Cognita, 2, (3), 320p. https://www.persee.fr/doc/geoly_0750-6635_1982_num_87_1_1513
31. Ménot, R.-P., Seddoh, K.F. (1980). Le massif basique stratifié précambrien de Djabatoure-Soutouboua (région centrale du Togo, Afrique de l'Ouest). Pétrologie et évolution métamorphique. Bulletin du B.R.G.M. 4(4) : 319–337.

 ISSN: 1857-7881 (Print) e - ISSN 1857-7431

https://www.researchgate.net/publication/260887781

32. Ménot, R.-P., Seddoh, K.F. (1985). The eclogites of Lato Hills (South Togo, West Africa): relies from early tectonometamorphic evolution of the Pan-African orogeny. Chemical Geology, 50, pp. 313–330. https://doi.org/10.1016/0009-2541(85)90126-3
33. Meschede, M. (1986). A method of discrimination between different types of mid-ocean ridge basalts and continental tholeiites with Nb-Zr-Y diagram. Chemical Geology, 56 : 207-218. https://doi.org/10.1016/0009-2541(86)90004-5
34. Middlemost, E.A.K. (1994). Naming materials in the magma/igneous rock system. Earth Science Reviews, 37 (3-4), pp. 215-224. https://doi.org/10.1016/0012-8252(94)90029-9
35. Nakamura, N. (1974). Determination of REE, Fe, Mg, Na and K in Carbonaceous and ordinary Chondrites. Geochemica and Cosmochimica Act, 38, 757-775. http://dx.doi.org/10.1016/0016-7037(74)90149-5
36. Sabi, B.E. (2007). Etude pétrologique et structurale du Massif Kabyè, Nord-Togo. Thèse Doctorat, FDS, Univ. Lomé, 256p.
37. Sabi, B.E., Gnazou, M.D.-T., Tairou, M.S., Togbé, K.A., Johnson, A.K.C. (2015). Granulitizsation of frontal nappes in the Kabyè massif in northern Togo. European Scientific Journal October 2015 edition vol.11, No.30 ISSN: 1857 – 7881. https://core.ac.uk/reader/236412410
38. Shand, S.J. (1943). Eruptive Rocks. Their Genesis, Composition, Classification and Their Relations to Ore deposits. 2nd edition, Murby London, 444p. https://www.scirp.org/(S(czeh2tfqyw2orz553k1w0r45))/reference/ReferencesPapers.aspx?ReferenceID=1945539
39. Sylvain, J.P., Collart, J., Aregba, A., Godonou, S. (1986). Notice explicative de la carte géologique 1/500.0000è du Togo, Mém. n°6, D.G.M.G./B.N.R.M., Lomé – Togo. https://scholar.google.com/scholar?q=+author:J.P.%20Sylvain
40. Tairou, M.S., Affaton, P., Sabi, B.E., Seddoh, K.F. (2009). Tectono-metamorphic evolution of the Mo and Kara-Niamtougou Orthogneic Suites, Northern Togo. Global Jour. of Geological Sciences, vol. 7, n°2, pp. 93-100. https://www.researchgate.net/publication/287411921
41. Tairou, M.S., Affaton, P. (2013). Structural Organization and Tectono-Metamorphic Evolution of the Pan-African Suture Zone: Case of the Kabye and Kpaza Massifs in the Dahomeyide Orogen in Northern Togo (West Africa). International Journal of Geosciences 04, 166-182. https://doi.org/10.4236/ijg.2013.41015

 ISSN: 1857-7881 (Print) e - ISSN 1857-7431

42. Tairou, M.S., Miningou, Y.M.W., Da Costa, Y.D., Kwekam, M. (2022). Petrostructural and Geochemical Characteristics of the Metamagmatites in the External Zone of the Dahomeyides Belt: Case of the Kantè Serpentinites (Northern Togo). International Journal of Geosciences, 2022, 13, 779-792. https://www.scirp.org/journal/ijg